Biomechanical Response of Glenoid Prostheses During the Use of Mobility Aids - A Finite Element Analysis

Submitted by:
Patrick S. Kroenung
Health Sciences

To

The Honors College

Oakland University

In partial fulfillment of the

requirement to graduate from

The Honors College

Mentor: Liying Zhang
Department of Biomedical Engineering
Wayne State University

Co-Mentor: Mary Bee
Department of Biology
Oakland University

February 15, 2017

Biomechanical Response of Glenoid Prostheses During the Use of Mobility Aids - A Finite Element Analysis

Abstract

Glenohumeral conformity, defined as the quotient of the radius of the humeral head and the radius of a glenoid implant, has been shown to be a critical factor of implant survivability following total shoulder arthroplasty (TSA). Several Studies have investigated the impact of glenohumeral conformity on stress-strain profiles, glenohumeral contact pressure, cement stress, and micromotions at the bone-cement interface. Biomechanical studies have centered around cyclic loading from low-force movements to make predictions regarding loosening of the implant and fixation failure. Total shoulder arthroplasty tends to be performed, however, on an aging demographic, subject to unique loading conditions regarding the shoulder complex. Specifically, the use of mobility aids, such as canes and walkers, function by transferring forces typically experienced by the lower limbs, to the upper limb. My Thesis will explore the mechanical effect of cane or walker usage on the fixation parameters that have been previously investigated, using an anatomically detailed finite element model of the shoulder. The results of this study could provide insight on optimal glenohumeral conformity in patients who use mobility aids, which may be different from the degree of conformity suggested based on generic shoulder movements. Varying degrees of conformity will be examined in two commercially available glenoid prostheses (Implant A, Implant B). Osteoarthritic shoulders often present moderate to severe retroversion, which is corrected by augmented material on the backside of the glenoid implant. The Implant A and Implant B implants vary in their augmentation geometry (Stepped vs Wedged) which may also impact the fixation criteria investigated by this study.

Background and Significance

Although most research regarding glenoid implant loosening centers around cyclic loading of low force humeral movements, several tasks resulting in high shoulder forces are recognized as plausible scenarios experienced by elderly individuals. High-force tasks investigated thus far include lifting a box (aprx. 5kg), picking up a suitcase (apx.10kg), sitting down onto a chair with the support of one's arms, getting out of a chair using one's arms, and walking with a cane (Anglin, 2000). The latter of these five scenarios is of particular interest as it would be repeatedseveral times per day, and on a daily basis. It was found that the average maximum glenohumeral contact force produced by walking with a cane ranges from .85 to 1.7 times body weight. Although the authors acknowledge that their values may somewhat overestimate glenohumeral contact forces, they are in rough agreement with other shoulder-biomechanics studies. Out of the 6.8 million Americans that use Assistive devices to aid in mobility, 6.1 million use walking aids such as canes, crutches, and walkers (Mobility Report 2000). The most prevalent ambulation aid used by the elderly, classified as 65 years or older, is the cane. Approximately 10.2% of the 65 and above age group uses a cane. (Mobility Report 2000).

There is no current research available on the co-occurrence of TSA and cane use, although the demographic and pathological trends in both ailments show clear convergence. Disability and resultant mobility deficits are projected to increase with growing populations of senior citizens (Bradley 2011). Between 1993 and 2007 the number of total shoulder arthroplasties increased by 10.6%. (Day et al. 2010). Canes are used by over 10% of people after the age of 65, and only increases with age. Total shoulder replacement rates peak in the 65-84 year-old age groups, with more than two thirds of all shoulder arthroplasties performed on patients 65 years of

age or older (Day et al. 2010, Dillon 2015, Kim 2011). The majority (58.5%) of mobility aid users are female (Mobility Report 2011). Procedure rates of total shoulder arthroplasty are consistently higher for women than men (Day et al. 2010, Dillon 2015, Kim 2011). Not only do both scenarios show convergence in patient demographics, they also show convergence in etiology. It is widely agreed upon that osteoarthritis is the most common cause (60-70.5% of all procedures) for total shoulder arthroplasty (Demographics and outcomes of Total Shoulder Arthroplasty p. 28, Dillon 2015). The 2nd and 3rd most common causes for the procedure are rotator cuff tear arthropathy and acute fracture or dislocation, with some variance in reported order. A review of 15,306 TSA procedures by the Australian national joint registry determined rotator cuff tear arthropathy as the second most common cause at 16.6% of all cases and fracture/dislocation at third with 8.1% of cases. Dillon and co-workers reviewed 6,336 cases and placed acute fracture as the second most frequent cause at 17% and rotator cuff arthropathy third at 15%. Although ambulation aids are prescribed for a broad spectrum of conditions, well outside of the scope of this study, osteoarthritis is the prominent condition associated with cane use (Mobility Report 2000). Cane use is commonly prescribed for arthritic conditions of the lower limb, which could aggravate the progression of osteoarthritis in the glenohumeral joint, as well as contribute to soft tissue pathologies such as destructive shoulder arthropathy (Bateni 2005). Cane use therefore does not only show converging trends in etiology with total shoulder arthroplasty, but is implicated as a possible cause of its pathology.

Walking aids of any variety (including canes) work by transferring weight form the lower body to the upper limb. Shoulder pathology results as force is transmitted to a joint that is not intended for weight bearing (Slavens, 2012). Superiorly directed forces can compromise the integrity of the glenohumeral joint through chronic vertical translation of the humeral head

(Newsam et al. 2003, Sharkey 1995). Even low-force superior migration of the humeral head has been strongly correlated to the degree of fixation failure (glenoid loosening) of the glenoid component of a TSA prosthetic system (Hopkins 2004, Franklin 1988). Increase in mechanical loosening is reported for larger components, due to a larger moment arm to the center of the implant when loaded eccentrically (Iannotti 2013). Modern glenoid implants are not symmetrical. The vertical axis presents an increase in moment arm from the center of the implant when compared to the horizontal. Directing forces in the superior direction would therefore also increase the length of the moment arm.

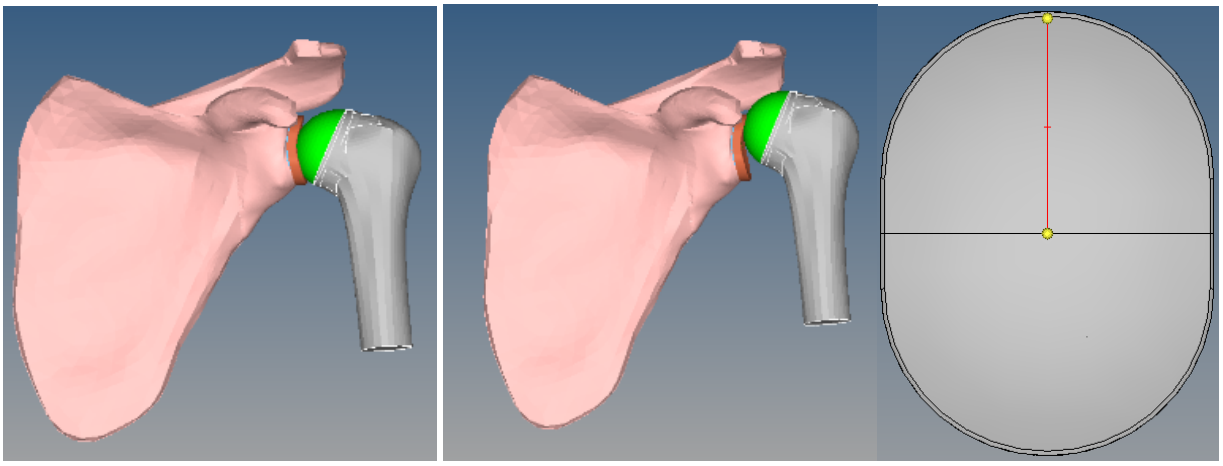

There is current debate about what degree of conformity (resulting from radial-mismatch) between the head of the humerus and glenoid implant provide optimal results when considering prevention of subluxation (and subsequent dislocation), normal shoulder kinematics, and fixation failure. (Anglin. 2000). When considering fixation failure evident by radiolucent lines a mismatch of 5.5mm or greater is considered best (Walch, 2002,). In regards to restoring natural shoulder kinematics a mismatch between 3 to 5mm is preferred (Karduna et al. 1997, Iannotti,1992). Forces comparable to cane use have only been investigated to determine the relationship of peak load and corresponding subluxation over five loading cycles. No studies

exist that examine the relationship between glenohumeral conformity and polymethamethacrylate (PMMA, the cement used in the fixation of the implant) in response to loading from mobility aids.

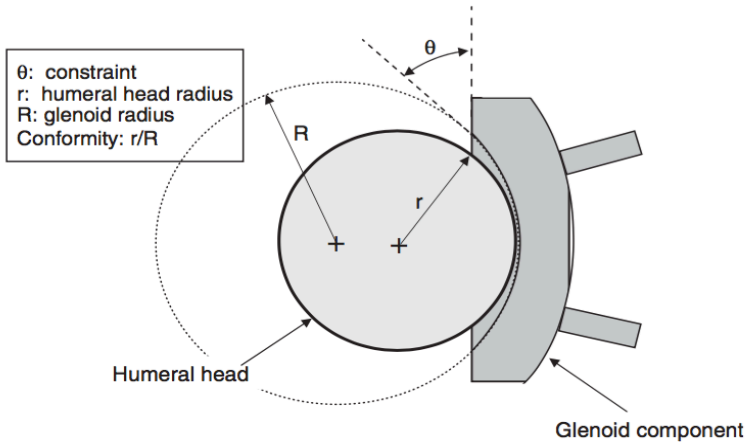

Fig. 1. Definition of conformity (i.e. ratio of humeral head radius over glenoid radius) and constraint (i.e. the maximum slope of the glenoid articular rim) in the glenohumeral joint.

(Hopkins, 2006)

Studies investigating the life span of PMMA cement are using glenohumeral contact forces well below what is experienced by individuals using mobility aids. When testing contact forces between the humerus and glenoid implant using finite element analysis, the force between the humerus and glenoid implant is modelled as a compressive force. The largest compressive for that has been investigated for cyclic fatigue cycling is 625N which corresponded to 85% body weight (Hermida, 2014). The use of a cane can produce contact forces of 170% body weight and may drastically increase the rate of loosening at the interface between PMMA cement and scapular bone. The difference in loading conditions induced by the use of mobility aids could warrant adjustment in the design parameters that are considered optimal.

Aims

1: Determine a range of glenohumeral conformity and constraint that does not pose a significant risk of subluxation of the glenohumeral joint.

2: Examine the influence of constraint on fixation criteria, specifically, implant stresses and micro-motion at the interface between the PMMA mantle and underlying polyurethane mounting block.

3: Estimate cement survivability by evaluating the cyclic fatigue life of the PMMA mantle as a function of its maximum principle stress. Compare two commercially available Implants in regards to their cement survivability.

Objectives

1: The glenohumeral joint is the most commonly dislocated joint (Hindle, 2013). The high rate of dislocation is assumed to result from the shallow depth of the glenoid surface (Hopkins, 2006). Joint depth is directly reflected in the radius of curvature of the glenoid surface. It stands to reason that when replacing the articular surface of the glenoid process, the articular surface of the glenoid implant would also dictate the rate of dislocation. Impact of conformity and radial mismatch on PMMA cement survivability should only be investigated within a range that does not pose a serious threat of dislocation. Therefore, conformity of the glenohumeral joint will be

progressively decreased by increasing the radial mismatch between the humerus and glenoid implant. Each implant will be tested over a range of radial mismatch from 1.0mm to 12.0mm. Each simulation will be monitored for humeral head translation, force ratio ($\frac{Subluxation\ Load}{Compressive\ Load}$), and time to subluxation.

2. Previous experiments have illustrated that decreasing conformity (increasing radial mismatch) leads to an increase in humeral head translation, whereas increasing constraint raises force ratios (Hopkins, 2006). Because less-conforming designs transfer more load to surrounding soft tissue before subluxation, the cement mantle should theoretically be subject to less stress (Anglin, 2000). The relationship between the aforementioned design parameters is in a delicate balance between risk of subluxation and fixation failure. This study will be the first to observe glenohumeral contact force, implant contact pressure, cement stresses, and micromotions in implants where no geometric features are changing other than conformity. Conformity will be changed by progressively scaling down the finite element model of the humeral head.

3: By estimating the cyclic fatigue life of the cement mantle, we can approximate which design configurations have the longest theoretical life-span. Significant differences in cement survivability could impact which implant to use for individuals utilizing mobility aids. If the fatigue life is significantly impacted by the conformity between the humeral and glenoid prostheses, the use of mobility aids may impact the size of humeral prostheses chosen for a shoulder replacement.

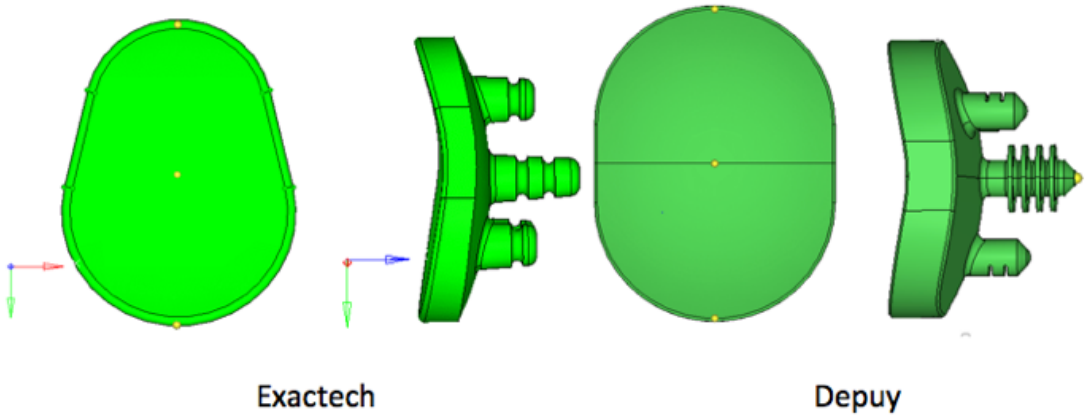

Methods

1: Various implants will be modelled as set into a polyurethane mounting block and exposed to a 750 N compression against a rigid modelled humeral head prosthesis. The Humeral head will be translated superiorly at a rate of 50mm/min. This method has since become the standard mechanical procedure for testing glenoid implants (ASTM-F2028-00). Further Analysis of subluxation has been re-created successfully using Finite element analysis (Hopkins, 2006). Using the PAM-SAFE (ESI Group, Paris, France) explicit finite element solver, Hopkins (2006) validated their model to within 4% of the experimental force ratios observed by Anglin (2000). Because this study is testing augmented glenoid implants using LS-DYNA (LSTC, Livermore, California) we will validate our results against the experimental data of both Anglin (2000) and Hopkins (2006).

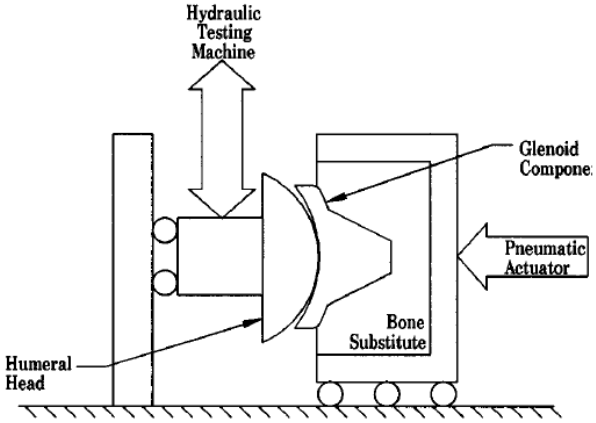

(Anglin 2000)

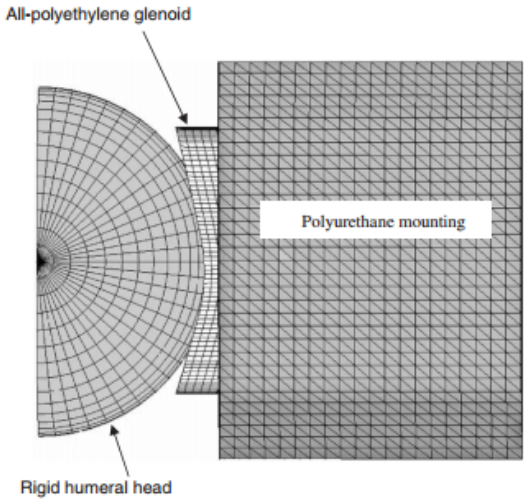

(Hopkins 2006)

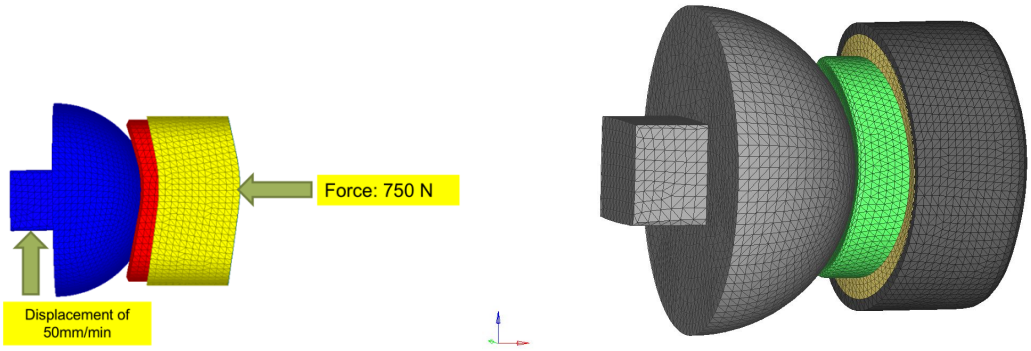

(Our Model)

To determine the point of subluxation, we will plot the resultant force of the humeral contact surface. Subluxation is the point immediately before the force vector of the humeral head will "jump" outside of the glenoid concavity. The subsequent dislocation will be marked by a significant decrease in the resultant force of the humeral head because the implant will no longer be resisting its movement.

A.R. Hopkins et al. / Journal of Biomechanics 39 (2006) 2476–2483

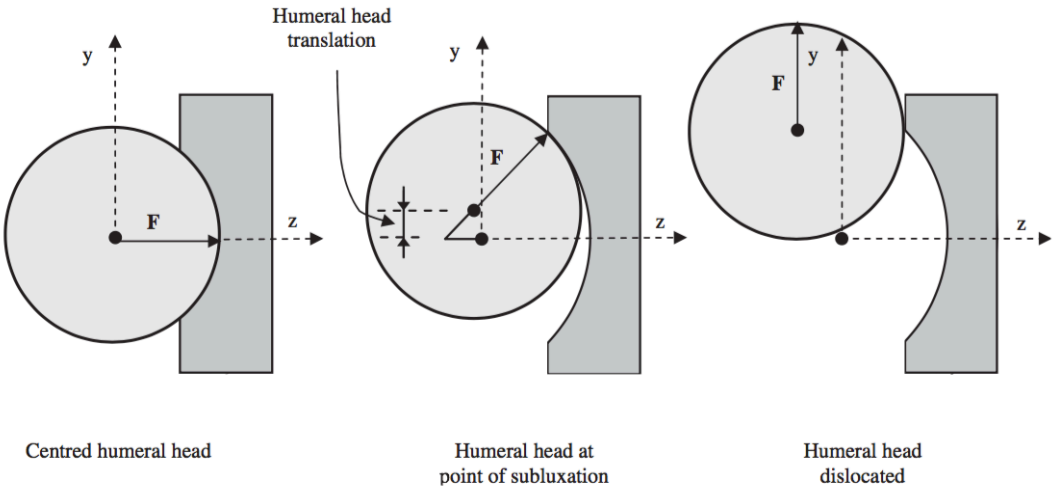

(Hopkins, 2006)

Force ratio (quotient of subluxation load divided by compressive load) as well as time to subluxation will be used to eliminate conformities that pose too great of a subluxation risk. Although our model is being validated against previous efforts, those studies tested several different implant designs that happened to differ in radius of curvature. Our experiment will test the same implants over a range of radial mismatches, by progressively scaling down the size of the rigid sphere representation of the humeral head.

2. The methods for Aim 2 will follow the same approach as Method 1. Variables investigated for Aim 2 will be cement stresses and micromotion at the articulation of the implant and polyurethane mounting block. Experimental data for these variables are automatically calculated and will be available as functions of LS-DYNA post processing. Contact will be modelled in LS-DYNA as Automatic Surface-to-Surface Contact. The resultant force of either contact surface can be retrieved and plotted in LS-post processing. Contact pressure of the polyethylene

implant component and maximum principle stress of the PMMA cement component are automatically calculated throughout the simulation. Micromotion contour plots will be generated from the relative displacement between nodes at the interface between the mounting block, cement layer, and implant.

3: Fatigue life will be predicted by a previously determined power of law function of maximum principle stress. Survivability of each finite element will be recorded over 10 million loading cycles. Cyclic fatigue life will be presented as the ratio of elements that survive to the total number of elements. The probability of survival (PS) for 10 million loading cycles will be given by:

$$PS = -A\sigma^3 + B\sigma^2 - C\sigma + D$$

Where σ is the maximum principle stress (MPa) that would generate a 95% probability of surviving 10 million loading cycles. A (.0005), B (.0202), C (.3304) and D (1.8365) are previously established constants for polymethamethacrylate (PMMA). (Murphy,Prednergast 2000)

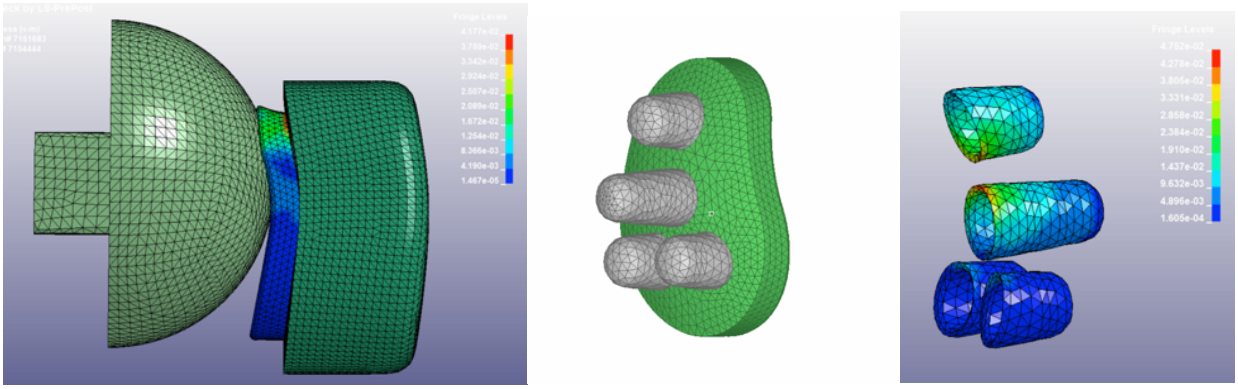

(Stress distribution visual from our pilot simulation)

Outcomes

The foundation of the proposed research is built on the validation of the finite element models that we will use to conduct our experiments. Because the Anglin mechanical test method (ASTM-F2028-00) has become the standard test method for humeral subluxation, our results should within 5% of the experimental data. The project at hand will not continue until the model is validated against previous data. Our results should indicate that decreasing conformity (radial mismatch) will increase the displacement distance of the humeral head under a constant loading conditions. When increasing the constraint of the implant the force ratio of horizontal compression and vertical shear is expected to increase. An increase in constraint is also expected to raise PMMA cement stresses and micro-motion at the interface between the polyurethane test block and cement mantle. The outcomes of this experiment will provide insight as to whether or not the optimal global design parameters of glenoid implants are applicable to the unique loading condition that cane use produces. Due to convergence of mobility aid use and TSA epidemiology, the loading condition this study examines is very relevant to glenoid implant loosening concerns.

Results of this study could provide insight into what form of mobility aid should be used post-operatively as well as long term. It may be beneficial for patients who rely on canes/elbow crutches to temporarily use axillary crutches or mobility aids that eliminate walking such as motorized scooters. If significant variation is seen between the Implant B and Implant A models it may be determined that one is less suitable for patients that already rely on aided ambulation. If cement stress values and micro-motions vary significantly between radial mismatch an optimal degree of conformity can be generated clinically by adjusting the radius of curvature of the humeral component.

Despite cane use and total shoulder arthroplasty affecting the same demographics, no epidemiological on their comorbidity exist. Further research will include integrating the implant models into a previously developed finite element model of the full shoulder complex, and running dynamic analysis that includes the complex motion of using a cane throughout the gait cycle. No previous studies exist on the scapulohumeral rhythm, glenohumeral contact force, and cohesive movement of the humerus through out a complete gait cycle while using a cane. In order to produce a dynamic analysis that resembles the natural biomechanics of cane use, a motion capture analysis using human subject will be required. Reverse total shoulder replacements are often used to prevent destructive arthopathy by reducing superior translation of the humeral head. Comparing anatomical and reverse total shoulder arthroplasty could offer additional criteria on which method may be used to restore the glenohumeral joint.

Aim 1 Finite Element Modelling

The purpose of aim one was to establish a range of glenohumeral mismatch that has a reduced risk of subluxation. Subluxation and dislocation are considered two of the main complications following shoulder arthroplasty (Oosterom, 2003). Many patients that require shoulder arthroplasty have compromised rotator cuffs, a condition only exacerbated by weight bearing. Due to a deficient rotator cuff the shoulder is often unable to provide a large enough stabilizing force to centralize the humeral head. Decreased stability in combination with high-load activity can lead to increased off-center loading. Off-center loading of the glenoid implant is the causing factor of joint subluxation and dislocation (Osterom, 2003). The key design features that impact the likelihood of eccentric loading are believed to be conformity and angle

of constraint. The most relevant measurement of glenohumeral stability is its force ratio at the point of subluxation (Anglin, 2000). While restraining movement of the humeral head is crucial to preventing subluxation, the joint must still allow enough translation to maintain adequate range of motion. The problem with designing a glenoid component is that the endoprosthesis has conflicting design parameters when considering range of motion and joint stability. Increasing range of motion for instance, also increased the eccentricity of loading (Oosterom, 2003). In order to analyze the impact that constraint and conformity individually have on force ratio and humeral translation, we have designed a test matrix that involves testing two implants with different constraint angles at five different radial mismatches. The Finite element model used was generated to resemble the ASTM-F2028-00 testing apparatus. Both the Implant B and Implant A Implants were modelled individually and then compared to the experimental results for a similar implant from Anglin's original experiment. Both implants had a standard (non-augmented) posterior face.

Schematic of ASTM-2028

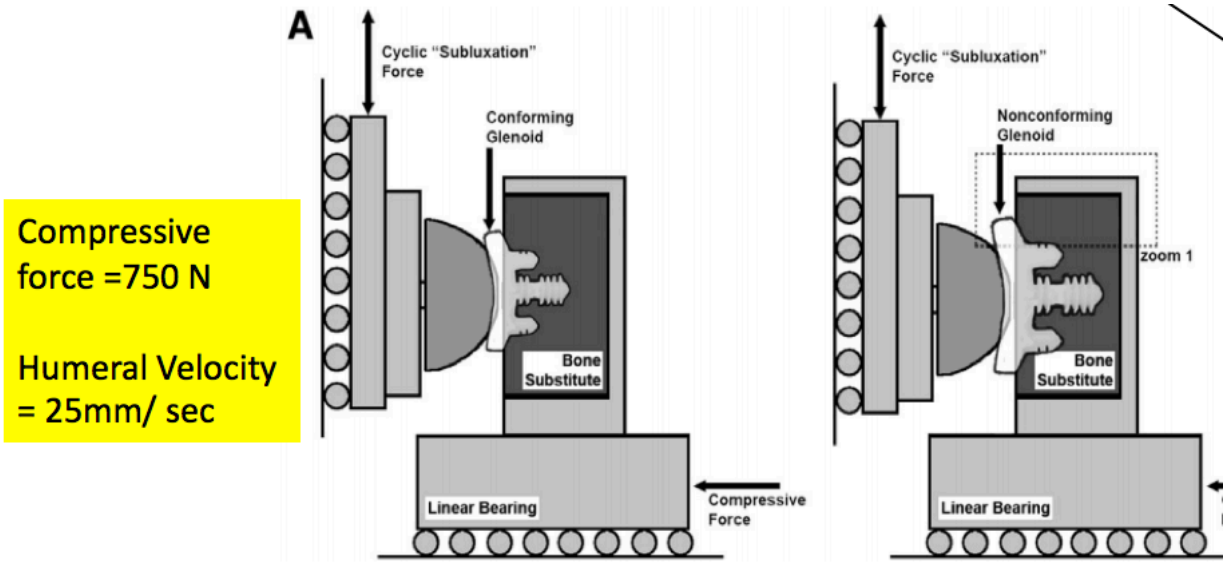

The mechanical test fixture applies a 750 N compressive force in the X-axis through the hydraulic actuator holding the mounted implant. The metal humeral component is translated superiorly at a speed of 25mm per seconds in the Z-axis. Subluxation is considered to be the point at which the humeral component contacts the rim of the glenoid implant, and at which point the resulting force is greatest. At any point following subluxation the Z-directional force should drop below its maximal value as the implant will deform and offer less resistance to the humeral head. Graphically, we can determine the subluxation point by tracking the Z-force contour plot of the humeral surface used in contact modelling. Maximal Z-force was always followed by a sudden drop in in force due to subluxation of the joint, as is theoretically described.

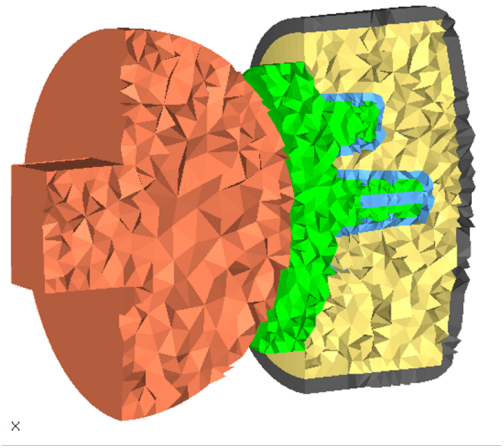

Mid Section View

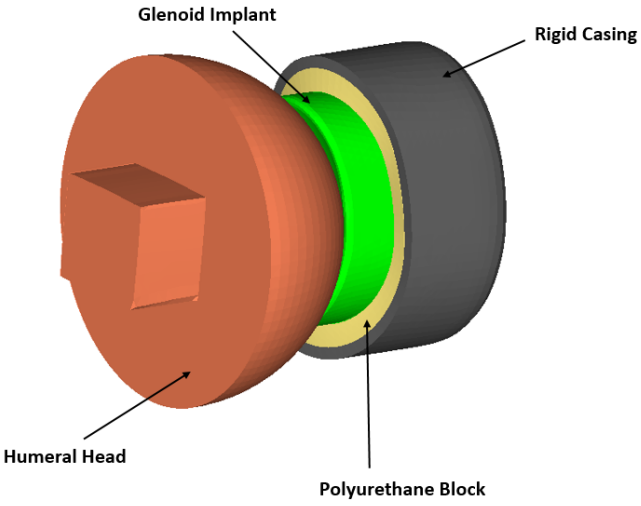

LS-DYNA Material Models for Implant B

Component Name	Material Card		
Humeral Head	MAT 20	Rho (Kg/mm3)	7.90E-06
		E (Gpa)	210
		Nu	0.3
Glenoid Implant (Polyethylene)	MAT 24	Rho (Kg/mm3)	1.00E-06
		E (Gpa)	1.26
		Nu	0.4
		Yield Strength (Gpa)	0.021
Cement (PMMA)	MAT 24	Rho (Kg/mm3)	1.00E-06
		E (Gpa)	2
		Nu	0.23
Mounting Block (Ployurethane)	MAT 57	Rho (Kg/mm3)	3.20E-07
		E (Gpa)	0.193

Table 1. Material cards and properties for Implant B implant.

Component Name	Material Card		
Humeral Head	MAT 20	Rho (kg/mm3)	7.90E-06
		E (Gpa)	210
		Nu	0.3
Glenoid Implant (Polyethylene)	MAT 24	Rho (kg/mm3)	1.00E-06
		E (Gpa)	0.52
		Nu	0.46
		Yield Strength (Gpa)	0.012
		Tangential Modulus (Gpa)	0.136
Cement (PMMA)	MAT 24	Rho (kg/mm3)	1.00E-06
		E (Gpa)	2
		Nu	0.23
Mounting Block (Polyurethane)	MAT 57	Rho (kg/mm3)	3.20E-07
		E (Gpa)	0.193

Table 2. Material cards and properties for Implant A Implant.

Hopkins, Andrew R., et al. "Finite element modelling of glenohumeral kinematics following total shoulder arthroplasty." Journal of biomechanics 39.13 (2006): 2476-2483.

In addition to modeling the implant, cement layer, humeral head, and hydraulic actuator, we had to create a custom model of the polyurethane block within which the implant was set. The polyurethane foam model is used because it has material properties that most closely represent trabecular bone (Shim, 2012). Not only are the material properties similar but their respective micro-architecture is nearly indistinguishable to a non-expert.

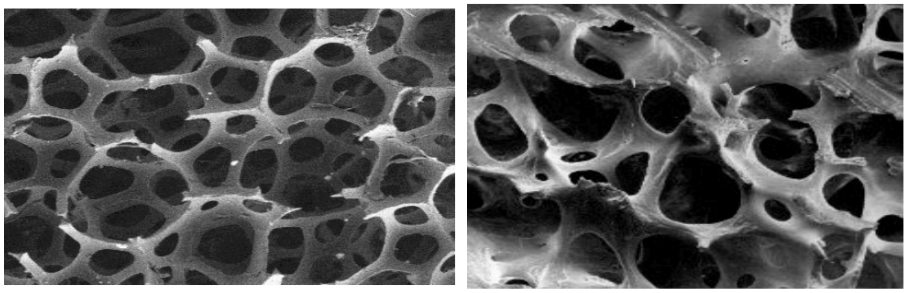

Polyurethane foam microscopic structure

Cancellous bone microscopic structure

(Shim, 2012)

Because foam material cards can include expansive ranges of moduli, we had to digitize and define a custom load curve into the MAT 57 material card. The polyurethane foam used as bone-substitute for the mechanical testing device had previously established stress-strain plots. The Area of contact between the polyurethane and PMMA bone cement was modeled with nodal connectivity, as was the area of contact between the implant and cement. Direct contact between the implant and polyurethane mounting block, as well as the humeral head and implant, is modeled as Automatic Surface to Surface.

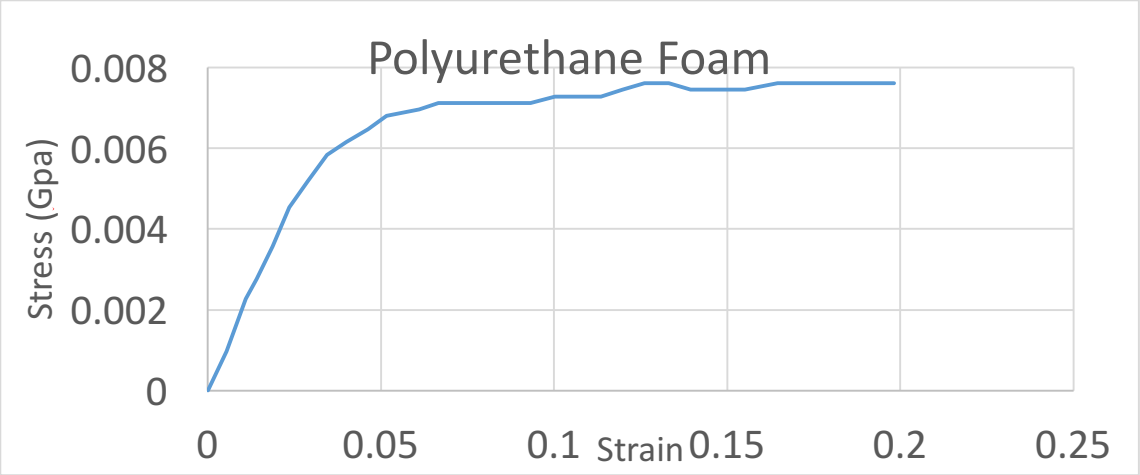

Foam Type : 6720 (ASTM standard F1839-08) used for trabecular bone

Kayla L. Calvert et al. J Mater Sci: Mater Med (2010) 21:1453–1461

Aim 1 Validation and Results

The experimental study that Anglin (2000) developed, which later became the ASTM-2028, tested a range of six commercially available glenoid implants. The humeral head in the experiment was kept constant, and the differences in radial mismatch merely resulted from the difference between each implant and the constant humeral head. In order to validated our FE model we had to compare it to the closest available implant analyzed in the Anglin (2000) study. One of the implants under investigation was a curved-back, peg-anchored implant with a 43° superior constraint angle. This prosthesis made a 3.5mm radial mismatch with the humeral head used in the experimental setup. The Implant A implant we are investigating closely resembles the mechanically tested implant. Due to differences in implant curvature, the humeral head in our model was scaled down in size to create the same radial mismatch (3.5mm). The Implant B implant was also investigated at a radial mismatch of 3.5mm but had a significantly lower

constraint angle. By testing both implants under the same condition we can see how significant of an impact constraint angle has on force ratio.

The force ratio that Anglin reported on the implant we chose to validate against was 0.72. The Implant A implant produced a force ratio of 0.729, whereas the Implant B implant was recorded at 0.691. These results illustrate the impact that constraint angle has on the Stability of the glenoid implant, with a greater force ratio indicating greater stability.

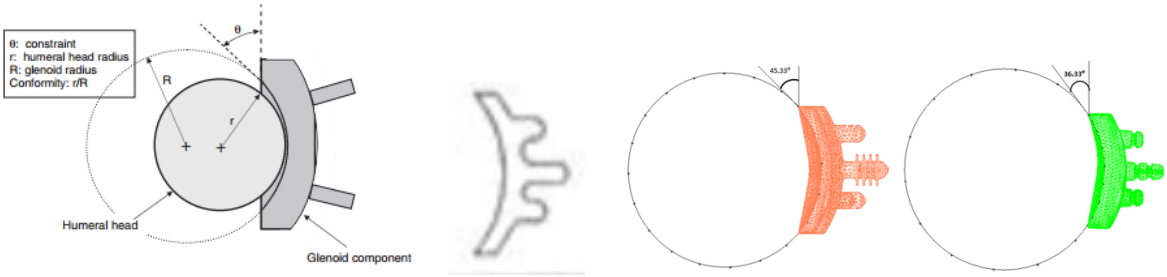

Characteristic	Anglin, 2000	Implant A	Implant B
Glenoid Radius (mm) , R	29.5	27	30
Humeral Head Radius (mm), r	26	23.5	26.5
Conformity r/R	0.88	0.87	0.88
Mismatch (mm), R - r	3.5	3.5	3.5
Superior Constraint Angle	43°	45.3°	36.3°

Table 4. Implant design features for Implant A, Implant B, and validation implant.

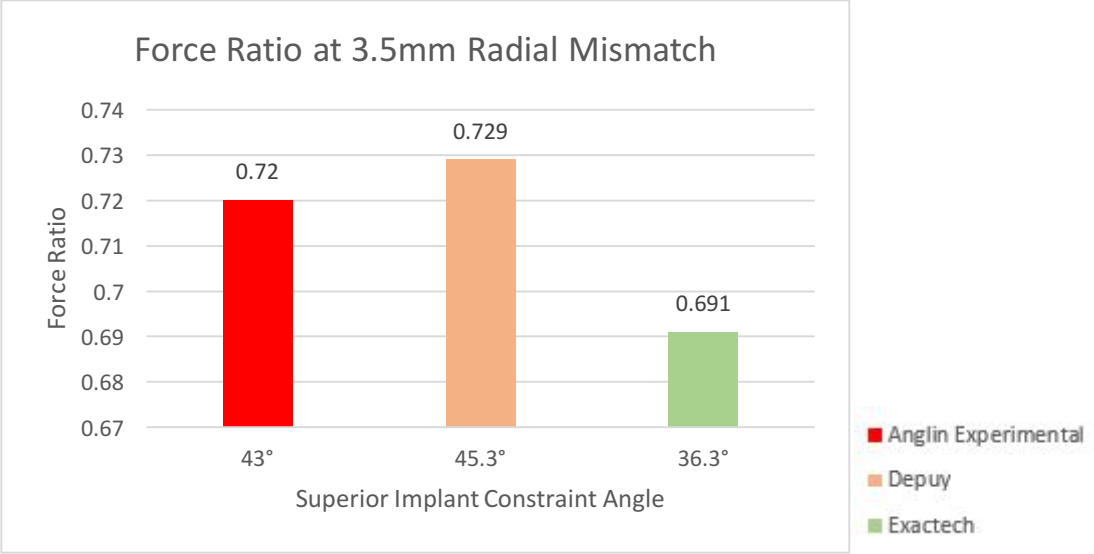

Figure 1. Force ratio comparison at 3.5mm radial mismatch

The Next step of our investigation progressively scaled the size of the humeral head in order to see if radial mismatch has a significant impact on the force ratio. Radial mismatch regulated conformity is the leading design feature in translation to the articular rim (Karduna et al, 1997). Karduna et al showed that prostheses with a glenohumeral mismatch of 3 to 5 mm most closely reproduced translation in natural shoulder joints. Other studies have shown however that fixation between the implant to the bone is greatest at a mismatch of 5.5mm or greater, with no decrease in clinical stability (Walch et al). We examined force ratio and humeral translation to isolate the impact of radial mismatch on each.

The experimental force ratios ranged from .677 to 7.46. The force ratios were higher for the Implant A implant and every single radial mismatch. There was no clear relationship between an increase in radial mismatch and an increase in force ratio. These results re-illustrate how much more of an impact constraint angle makes on the stability of the prosthetic joint than the radial mismatch between its two components.

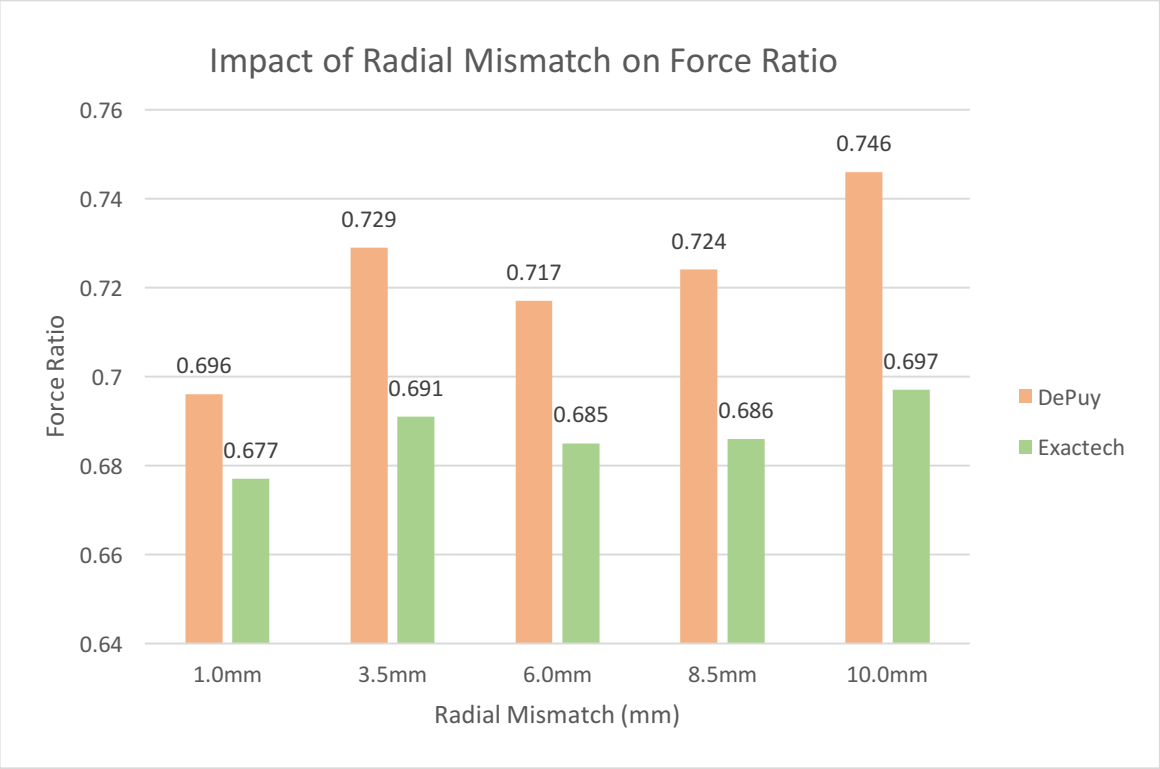

Figure 2. Force ratio at variable mismatch.

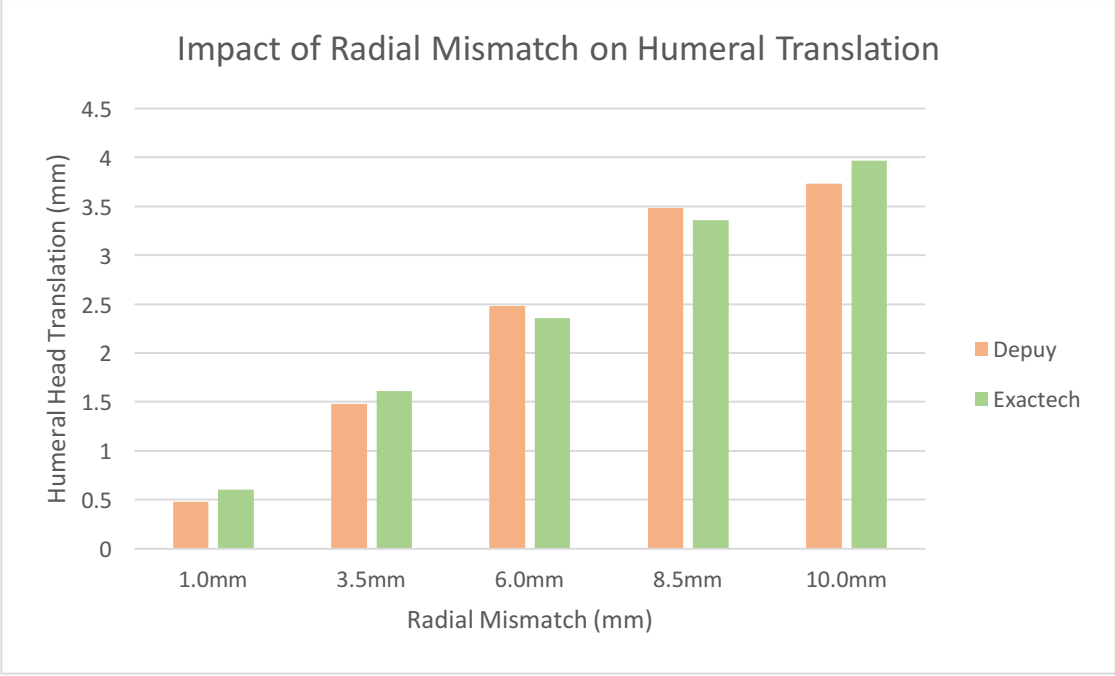

Figure 3. Humeral translation at variable mismatch

Although The force ratio did not change greatly in its maximal values (the point of subluxation) the point at which they occurred did. There is a clear trend in the translation of the humeral head with an increase in mismatch. It was expected that we would see an increase in force ratio with an increase in constraint and an increase in translation with an increase in mismatch (Hopkins, 2006). What is surprising is how mutually exclusive the two design elements are. The degree of superior constraint angle made no distinguishable difference in the displacement value of the humeral head. In the simulations it was evident that with a further translation lead to greater implant deformation due to the eccentricity of the humeral head.

Aim 2 Stress Distribution Results

Von Mises stress patterns which combine any set of shear, normal, and bending stresses were selected in order to compare overall stress distribution as a function of radial mismatch. The current study was not intended to estimate failure in the polyethylene implant, but to gain theoretical understanding of the wear pattern induced by variation in radial mismatch. Several studies of retrieved glenoid components show erosion of the articular rim as well as component fracture due to polyethylene deformation in vivo (Swieszkowski, 2003).

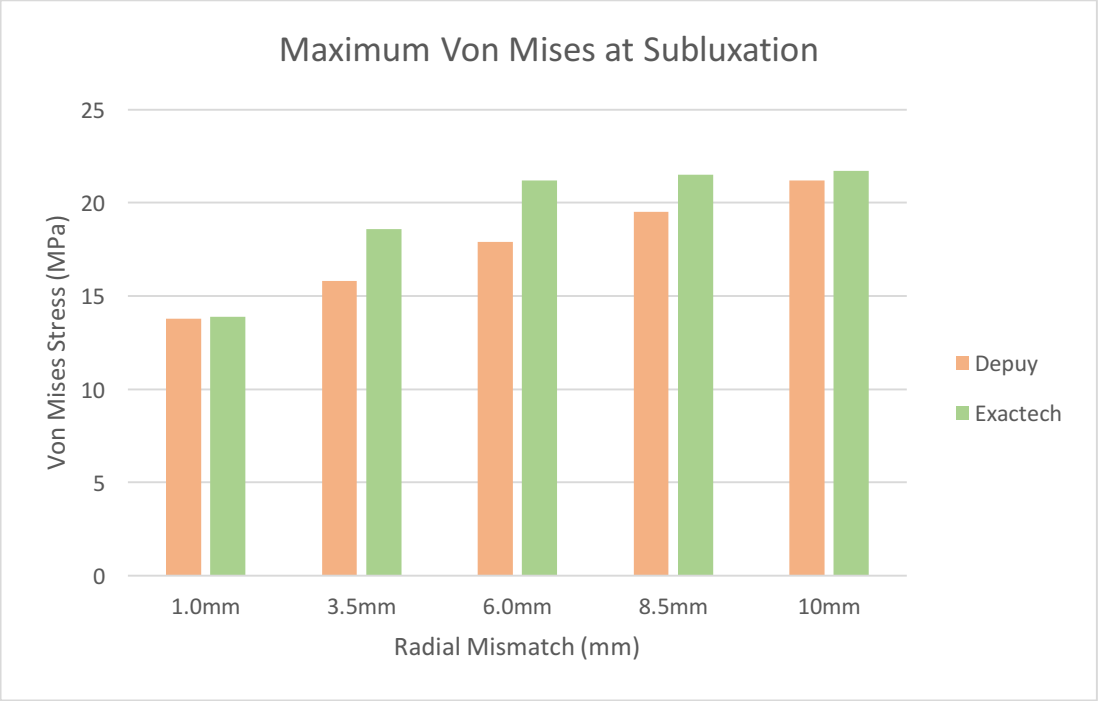

Figure 4. Maximu Von Mises at variable mismatch.

With increasing radial clearance, the area through which the contact force was applied became smaller. Stress increases with a decrease in the area through which a force is applied, so it is reasonable that the maximum stress increased with an increase in radial mismatch. Von Mises values ranged from 13.8 to 21.7 MPa. Stress values were higher in the Implant B model for every radial mismatch. The yield strength of ultra high molecular weight ranges from 20 to 26 MPa (Kurtz, 1998). Four of the implants under investigation had elements brought to critical values of polyethylene failure. The Implant B model exceeded values for plastic deformation at 6, 8.5, and 10mm of radial mismatch. The Implant A implant exceeded 20 MPa only at 10mm of radial mismatch. The total volumetric failure of these implants was calculated at the subluxation point.

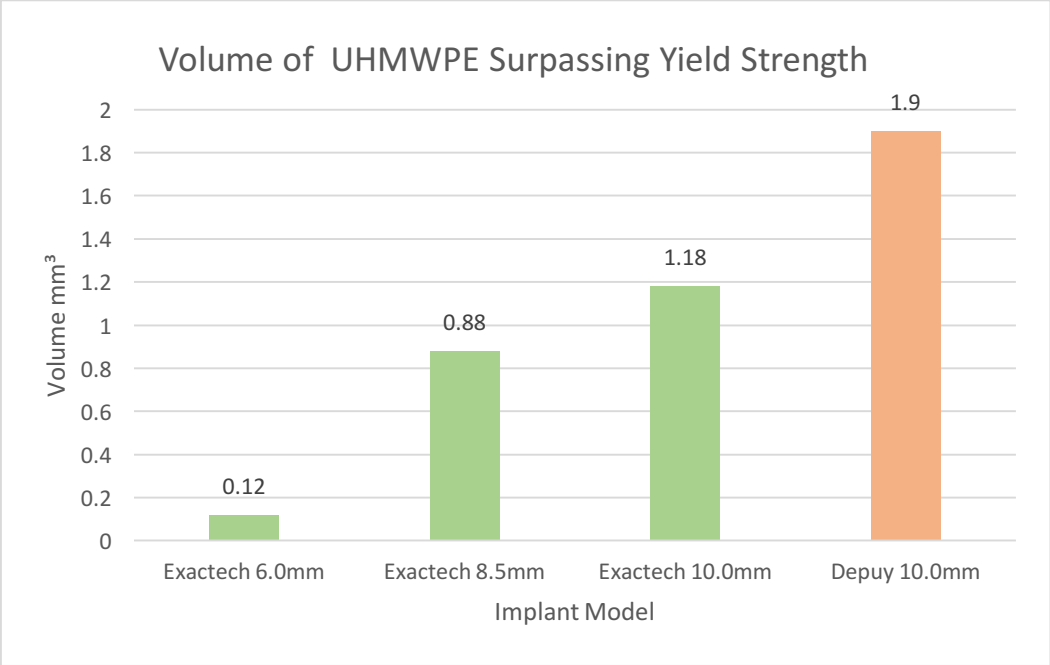

Figure 5. Volume of failed polyethylene.

In the Implant B models the volume of failed elements increased with increasing radial mismatch. Volumes of failure in the Implant B model ranged from .12 to 1.18 cubic millimeters. Although the volume of failed elements is extrememly low, this could indicate crack formation. Only one Implant A model (10.0mm) contained elements that reached the yield strength for ultra high molecular weight polyethylene. The Implant A model had a volumetric failure of 1.9 cubic millimeters. Although the contact area became smaller by increasing radial mismatch, the surface area exposed to high quantities of stress increased. The Stress distribution also became more and more eccentric with increasing humeral clearance, due to the increased distance of permitted translation.

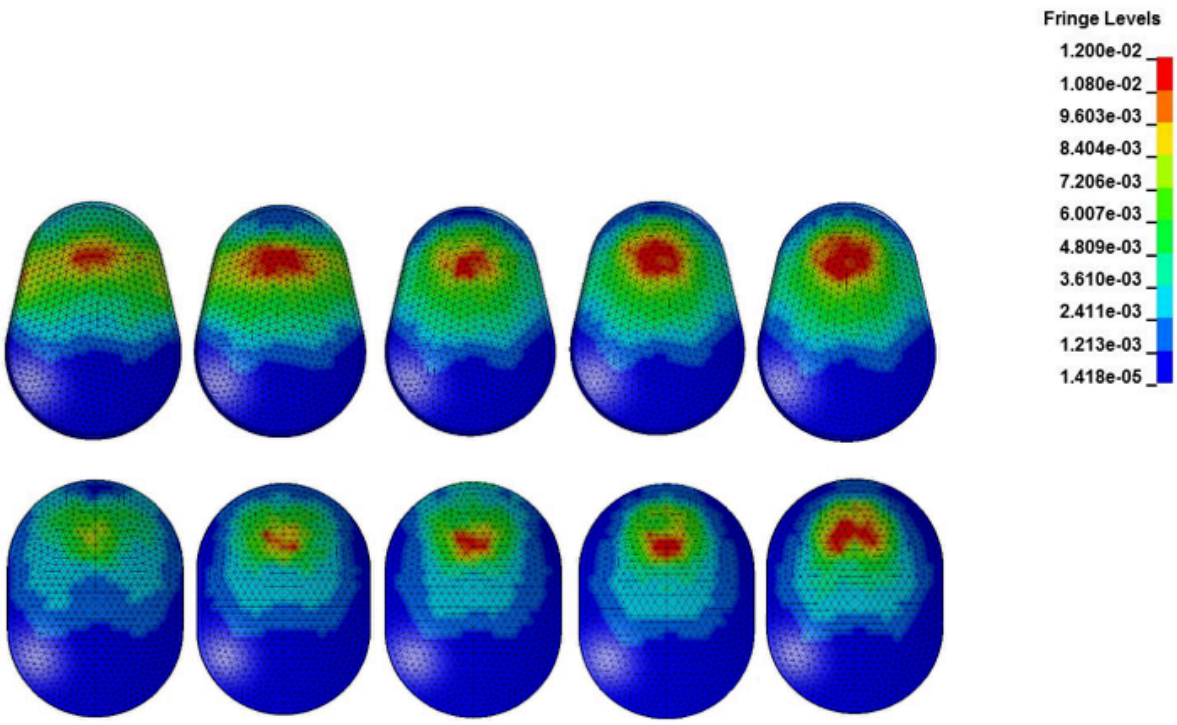

Stresses that do not surpass the yield strength of polyethylene can still be of concern as this load can be applied hundreds of times per day for some one using a cane. Areas of elevated stress were larger in the Implant B model at each radial mismatch. Methodology for assessment of micro-motion is possible in LS-DYNA but were not included in this study. Upon post processing it was determined that the oscillations in the model made it too difficult to validate nodal movement in microns, as the changes from vibration often did not correspond with the exact millisecond of subluxation in the output file (d3plot). The result of this was that although there was a movement trend in one direction, at certain points the nodes would record negative directional movement. Now that subluxation points have been determined for each model it will be possible to run the model only to subluxation point with a higher output frequency and slower speed without much cost in computational time. Future simulations will hopefully produce

results that we can validate against experimentally determined micro-motions. Pilot simulation thus far have produced promising results.

Aim 3 Results

Cement stress comparisons have only been performed at 3.5mm of radial mismatch. Due to high stability and low implant stress 3.5mm of mismatch has optimal values for performance criteria evaluated thus far. Clinical recommendations suggest a mismatch between 3 and 5 mm and therefore the 3.5mm mismatched model is most likely to be used clinically out of our experiment series. The peak maximum stress values between the Implant B and Implant A model were calculated at subluxation point. Peak maximum principal stress was 10.72 MPa for Implant B and 13.4 MPa for Implant A.

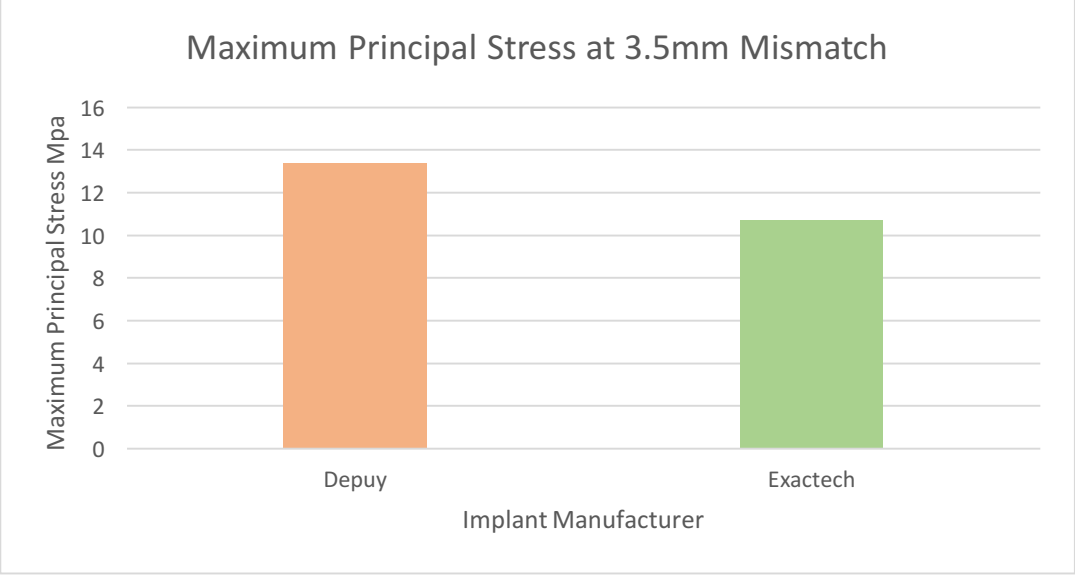

Figure 6. Maximum principle stress of PMMA

Although maximum principal stress was higher in the Implant A models, the number of elements experiencing elevated levels of stress was lower. Cyclic fatigue life of PMMA for 10 million cycles has been previously derived into a power of law function by Murphy and Prendergast in 2000. The power of law function is $Ps = -A\sigma^3 + B\sigma^2 C\sigma + D$ Where Ps is the probability of survival, σ is the maximum principal stress (MPa), A = .0005, B = 0.0202, C = 0.3304, and D = 1.8365. (Murphy, Prendergast, 2000) Using this equation to set the failure criteria for a volumetric failure fraction of the entire polymethamethacrylate cement layer, we can estimate the volume of cement that would survive 10 million cycles. (Murphy, Prendergast, 2000)

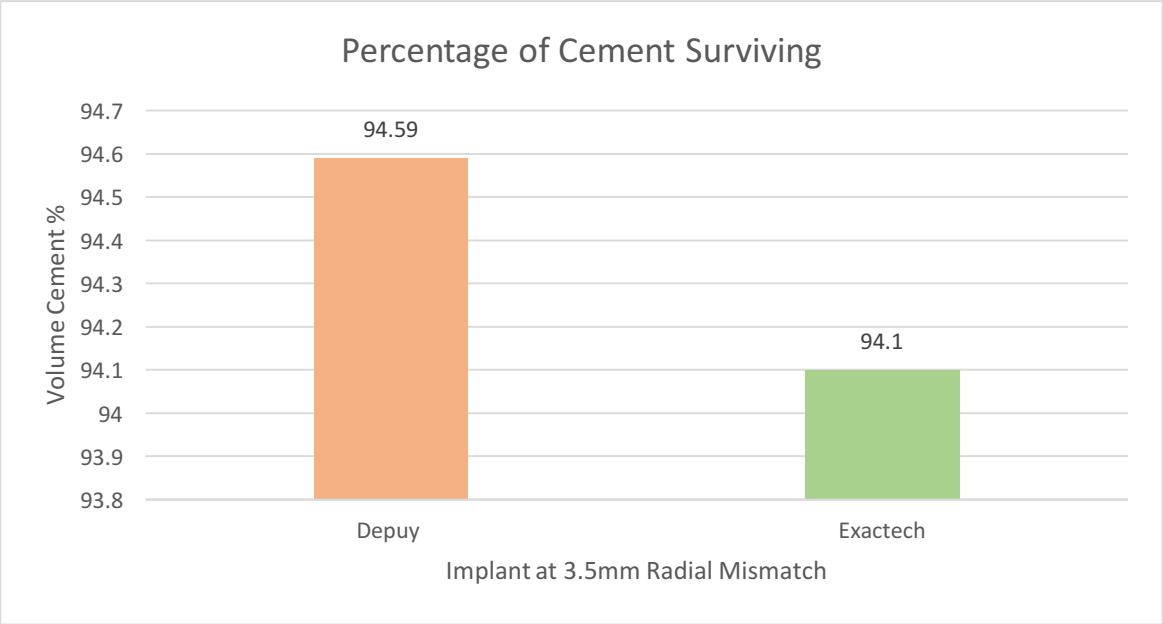

Figure 7. PMMA survival fraction

Both Implant A and Implant B had cement survivability above 94% after 10 million cycles. The two implants did however have variation in their cementation technique, leading to different

volumes of cement. By applying the fraction of elements above critical threshold to the volume of cement, we can derive the volume of cement that would fail to survive 10 million cycles.

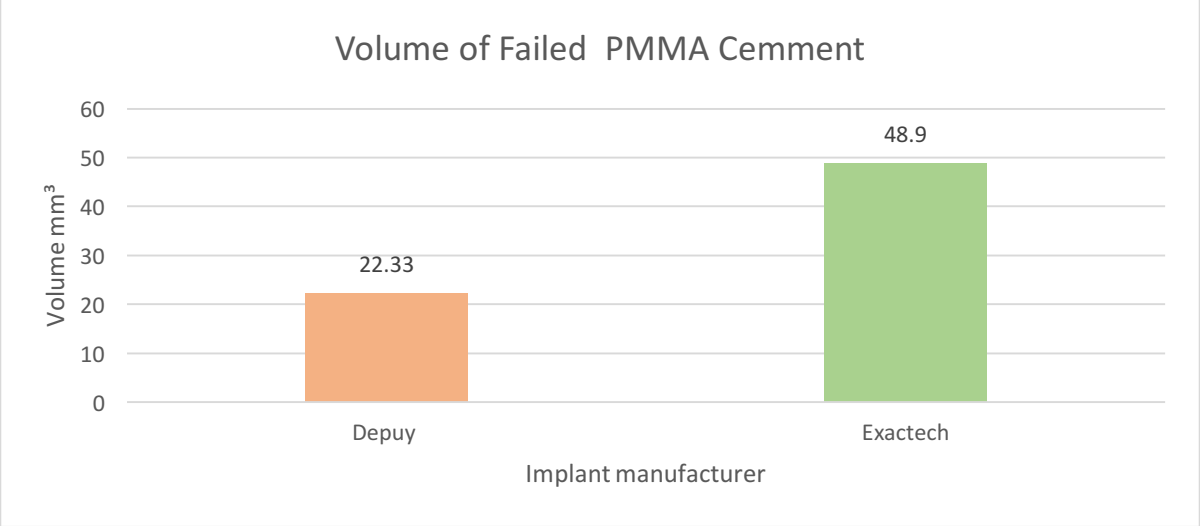

Figure 8. Volume of failed PMMA

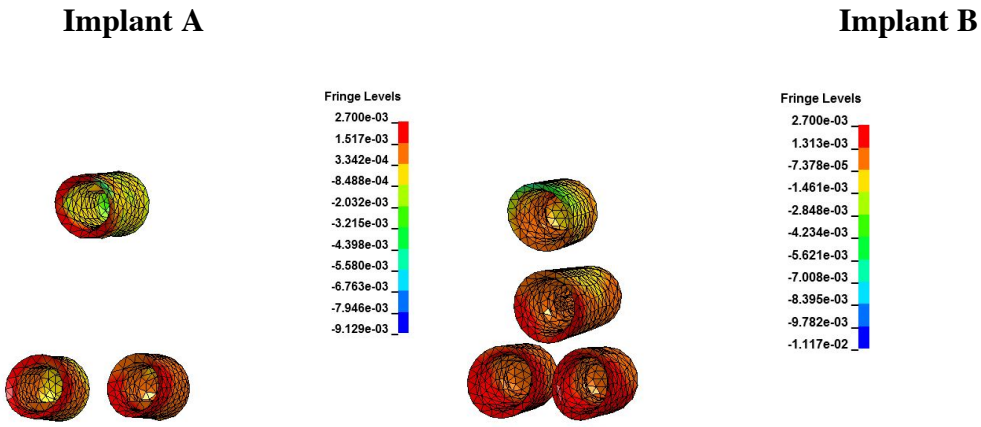

The stress distribution pattern of failed elements was similar for both implants. The majority of failed PMMA was localized to the cement surrounding the inferior pegs. The inferior peripheral pegs are contralateral to the path of loading from the humeral head. Critical stress values are closest to the contact surface between PMMA cement and the polyethylene pegs embedded within.

Discussion

In the validation simulation that compared Anglin's experimentally determined force ratio to our model, we are able to reproduce the results with high accuracy. Our force ratio elevation of .09 could be attributed to the fact that our constraint angle was 2.3º greater. It was predicted that increasing the radial mismatch (decreasing conformity) should reduce the force ratio, decreasing the force required to sublux and subsequently dislocate the joint (Anglin, 200, Hopkins, 2006). Although variations occurred in force ratio there was no identifiable trend that could be reduced down to the change in radial mismatch. At every single radial mismatch however the implant with the greater constraint angle displayed a higher force ratio. The contradiction between our simulation and experimental studies could be the fact that no previous study controlled radial mismatch through scaling the size of the humeral head. Previous studies that examined radial mismatch did so across a wide range of implant designs, constraint angles, thickness, and sizes. Implicating glenohumeral mismatch as a causation for changes in force ratio across a range of prostheses with so many variables is not feasible. Clinically, radial mismatch is more commonly determined by the selected size of the humeral component, as the size of the glenoid component should not exceed the diameter of the glenoid surface itself. By scaling the humeral head our study was the first to examine the isolated impact of radial

mismatch on force ratio. Results of our simulations indicate that the constraint angle of the slope on which the humeral component translates, has a much larger role in controlling force ratio than the degree of mismatch. Increasing constrain angle increased the subluxation force value, providing a greater resistance to dislocate the joint. The progressive increase in glenoid clearance did have a positive relationship with the displacement distance of the humeral head at subluxation. The exact translational distance that would be considered unstable has not yet been determined. Although there was no way to determine a translational value that would make a radial mismatch unsafe, we were able to do so based on the yield criteria of the implant.

As predicted by several studies a decreased contact area would concentrate force leading to higher Von Mises stress values (Friedman 1992, Anglin 2000, Hopkins 2006). At a radial mismatch greater than 6.0mm all of the Implant B models contained elements that surpassed the yield strength of the polyethylene (UHMWPE) component. Implant A models did not reach this threshold until 10.0mm of radial mismatch. Due to the fact that 3.5mm of radial mismatch is within the current clinical recommendations, and both models were within elastic limits, further comparisons occurred only at 3.5mm.

A research group out of California was the first to use Murphy and Prendergast's cement survivability equation in the finite element analysis all polyethelyne glenoid components (Hermida, 2014). PMMA cement is crucial in these implants since they do not contain any metal screws. Hermida used a force of 625 N that was modelled as a static compressive force into the center of the implant. The force was intended to reproduce the same in vivo measurements of glenohumeral joint reaction forces that were reported by Anglin. These force values are intended to model high load activities such as weight bearing on a cane. The stress values that Hermida reported however, do not take into consideration that weight bearing from cane support produces

a dynamic load scenario in the shoulder. The Hermida et al. study also estimated that someone with a glenoid prosthesis may perform up to 25 activities per day that cause this amount of stress on the implant, bone, and interfacial cemment. The reality is that someone who depends on a cane or forearm crutch for aided ambulation would be exposed to this level of stress hundreds of times per day. Even a sedentary adult in in the America is estimated to take approximately 1,000-3,000 steps per day. For some one using a cane 10 million cycles would only represent approximately 10 years, not counting any other high load activities. At 10 million cycles both implants showed a cement volume failure at greater than 5%. Hermida et al. did not report the exact value of cement for their standard glenoid (A and C), but their graphical depiction is close to 100%.

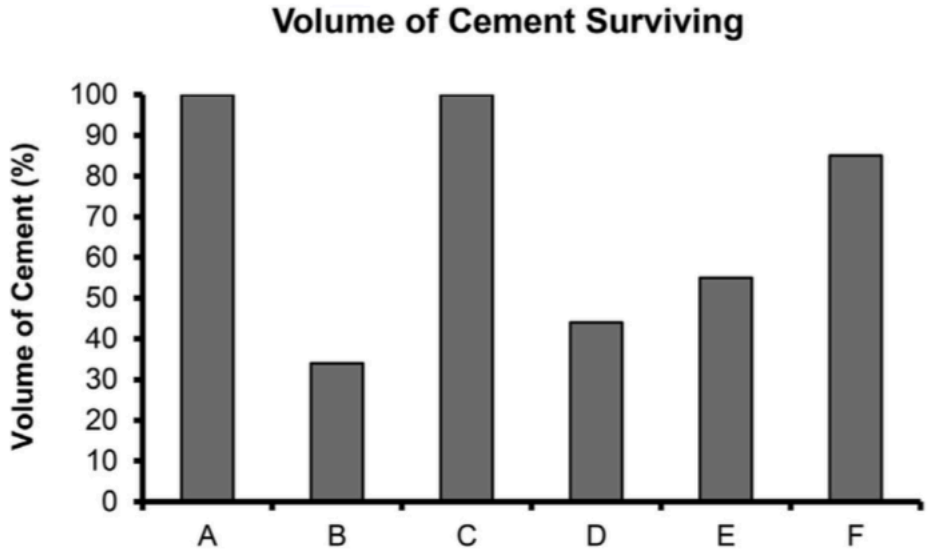

(Hermida et al., 2014)

Reproducing the dynamic motion of superior translation clearly decreased the amount of surviving cement. Taking a volumetric failure measurement at the time of initial compression almost none of the cement would fail in our model either. In the time it takes to reach

subluxation stress values in the cement mantle increase dramatically. Our experiment shows that using static loads to reproduce dynamic movements does not appropriately represent the stresses experienced by the components whose failure is implicated in implant loosening.

An interesting discovery was discrepancy between stress distribution in the implant and PMMA components. Polyethylene is a relatively ductile material, whose failure is estimated using Von Mises stress, due to the brittle nature of polymethamethacrylate its primary criteria in failure analysis is maximum principle stress. Using their respective stress criteria, we can se that as the humeral head translates superiorly, the majority of the failing cement is localized to the contralateral peripheral pegs (inferior).

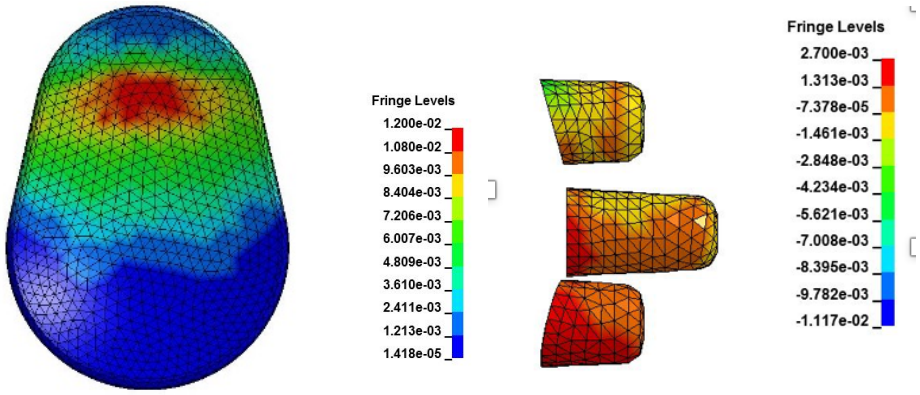

The loosening of a contralateral peg in response to eccentric loading should have a significant impact in the amount of edge liftoff experienced by the implant. This phenomenon is a major concern in glenoid stability and is often referred to as the "rocking horse" phenomenon (Karelse, 2015). Further investigation into the micro-motion of the glenoid rim contralateral to the path of loading, will potentially elucidate a direct relationship between the degree of constraint angle, and the likelihood of experiencing the rocking horse phenomenon.

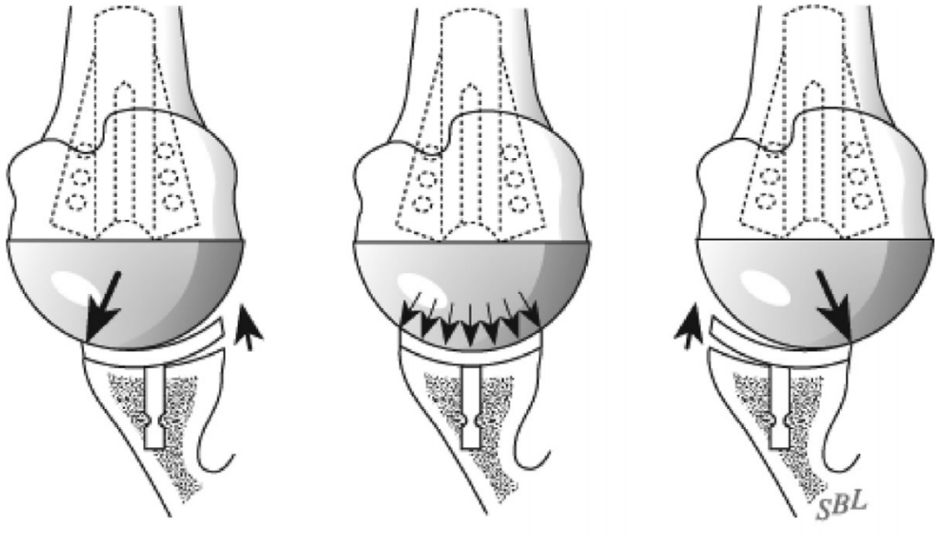

(Matsen, 2008)

Due to the amount of simulation we have run so far a full statistical analysis has not been completed but is currently in process. Simulations that incorporate the glenoid implant into a full musculoskeletal model of the scapular complex are also currently under way. Aside from investigating glenoid constraint and conformity, future investigations will include augmentation size as well as shaped.

Autobiographical Note

The road to the research projects I am currently involved with developed over the course of pursuing interests that were not entirely congruent with my formal education. The journey began through my interest human anatomy and biomechanics while I was pursuing a pre-physical therapy major. Interest in anatomy drove me to begin working as a teaching assistant and supplemental instructor for the undergraduate anatomy courses at Oakland university. After several semesters I began working as a teaching assistant at the Oakland-Beaumont Graduate Program of Nurse Anesthesia, The Eugene Applebaum Physician's Assistant prgroam at Wayne State, and Continuing Education for Occupational Therapists at the University of Detroit Mercy. Having substantial experience with cadaveric dissection I was hired on by the Injury Biomechanics Research Center (IBRC) at the Ohio State University's College of Medicine as an undergraduate research assistant. The IBRC consists of both the Injury Biomechanics Research Lab as well as the Skeletal Biology Research Lab, both of which heavily rely on injury data acquisition from post mortem human surrogates (cadavers). The majority of the research performed at the IBRC centered around injury response in high force trauma such as motor vehicle crashes, athletic injuries, and underbody explosions in military settings. Over the course of the summer I worked on several projects for The Transportation Research Center (TRC), the National Highway Traffic Safety Administration (NHTSA), and the Department of Defense (USDOD). Much of the work required gathering of anthropometric data from computed tomography images and bone quality assessment using Dual-energy X-ray Absorptiometry, at which point I developed an interest in biomedical imaging in orthopaedic research. Upon my return to Michigan I was referred by my previous primary investigators to the Wayne State

Department of Bioengineering. Having experience in data acquisition from medical imaging files I was offered a position at the Advance Human Modelling Laboratory (AHML), which specializes in the generation and validation of finite element models of the human body for the use in crash analysis. Because my mathematics background does not extend beyond statistics and pre-calculus I was initially accepted on a volunteer basis to become more familiar with FEA and the software (Hypermesh and Ls-Dyna) used by the lab. Since then I have been trained and certified by Altair in the use of Hypermesh, and taught by the graduate students in the lab to be proficient in the use of LS-Dyna. I will now be working at the AHML as a paid research assistant as part of a larger project investigating shoulder prostheses for the Orthopaedic Research and Education Foundation (OREF). Due to a lack of formal education in Finite Element Analysis, all modelling and analysis for my thesis is 1. Reviewed by my partner (Masters in Mechanical Engineering student) 2. Validated against published data 3. Reviewed by my employer and mentor Dr. Liying Zhang. One of the reasons I wanted to work on the glenoid implant model is because further down the line I hope to be performing the procedure. Total shoulder arthroplasty is of particular interest to me due to the fact that it has the highest rate of complication out of any major joint surgery.

If accepted to the MD/PhD programs to which I am applying, I would like to focus my research on skeletal biology, specifically developing more accurate finite element models of human bone. Bone is often grossly simplified as an isotropic linear elastic despite being a very complex composite material that does not display direction-independent mechanical properties. My goal is to work on methods that allow for the generation of individualized finite element models from CT scans, that allow for a variety of implants and their pertinent design features to be tested preoperatively. Individual anthropometry could be used within the design process of

personalized implants, rather than to reshape bony structures to accommodate a standardized prosthesis.

References

Allred JJ, Flores-Hernandez C, Hoenecke HR and D'Lima DD. Posterior augmented glenoid implants require less bone removal and generate lower stresses: a finite element analysis. *J Shoulder Elbow Surg* 2016; 25: 823–30.

Anglin, C., Wyss, U., & Pichora, D. Glenohumeral contact forces during 5 activities of daily living. *Journal of Engineering in Medicine* 2000; 214(6):637-44.

Anglin, C., Wyss, U.P., Pichora, D.R. Shoulder prosthesis subluxation: theory and experiment. *Journal of Shoulder and Elbow Surgery* 2000; 9 (2), 104–114

Bradley S., and Hernandez C., 2011.Geriatric Assistive Devices. *Am Fam Physician*. 2011; 84(4):405-411.

Day J.S., Lau E., Ong K.L., Williams G.R., Ramsey M.L., Kurtz S.M. Prevalence and projections of total shoulder and elbow arthroplasty in the United States to 2015. *J Shoulder Elbow Surg*. 2010; 19(8):1115–1120.

Dillon M.T., Ake C.F., Burke M.F., Singh A., Yian E.H., Paxton E.W., Navarro R.A.. The Kaiser Permanente shoulder arthroplasty registry: results from 6,336 primary shoulder arthroplasties. *Acta ortopaedica* 2015; 85(3).

Franklin J.L., Barrett W.P., Jackins S.E., Matsen F.A. Glenoid loosening in total shoulder arthroplasty—association with rotator cuff deficiency. *J Arthroplasty* 1988;3:39-46.

Gregory T.M., Sankey A., Augereau B., Vandenbussche E., Amis A., Emery R., et al. Accuracy of glenoid component placement in total shoulder arthroplasty and its effect on clinical and radiological outcome in a retrospective, longitudinal, monocentric open study. *PLoS One*.2013;8:75791.

Hermida J.C., Flores-Hernandez C., Hoenecke H.R., D'Lima D.D. Augmented wedge-shaped glenoid component for the correction of glenoid retroversion: a finite element analysis. *J Should Elb Surg*.2014;23:347–54.

Hindle P., Davidson E.K., Biant L.C., et al. Appendicular joint dislocations. *Injury*. 2013; 10:1016

Hopkins A.R., Hansen U.N., Amis A.A., et al. 2006. Finite element modelling of glenohumeral kinematics following total shoulder arthroplasty. *J Biomech* 39:2476–2483.

Iannotti J.P., Lappin K.E., Klotz C.L., Reber E.W., Swope S.W. Liftoff resistance of augmented glenoid components during cyclic fatigue loading in the posterior-superior direction. *J Shoulder Elbow Surg* 2013; 22(11): 1530-6.

Iannotti J.P., Gabriel J.P., Schneck S.L., Evans B.G., Misra S. The normal glenohumeral relationships. An anatomical study of one hundred and forty shoulders. *J Bone Joint Surg Am*

1992;74:491-500.

Kaye H.S., Kang T., LaPlante M.P. Mobility device use in the United States. Disability statistics report no. 14. Washington, DC: National Institute on Disability and Rehabilitation Research, U.S. Department of Education; 2000.

Karduna, A.R., Williams, G.R., Williams, J.L., et al. Glenohumeral joint translations before and after total shoulder arthroplasty. A study in Cadavera. *Journal of Bone and Joint Surgery* 1997; 79 (8), 1166–1174.

Kim S.H., Wise B.L., Zhang Y., Szabo R.M. Increasing incidence of shoulder arthroplasty in the United States. *J Bone Joint Surg Am*.2011 93(24):2249–2254.

Kurtz S.M., Pruitt L., Jewett C.W., Crawford R.P., Crane D.J., Edidin A.A. The yielding, plastic flow, and fracture behavior of ultra-high molecular weight polyethylene used in total joint replacements. *Biomaterials* 1998;19:1989-2003.

Matsen F.A., Clinton J., Lynch J., Bertelsen A., Richardson M.L. Glenoid component failure in total shoulder arthroplasty. *J Bone Joint Surg Am*. 2008;90:885–96

Murphy B.P., Prendergast P.J. On the magnitude and variability of the fatigue strength of acrylic bone cement. *Int J Fatigue* 2000;22:855-64.

Newsam, C. J., Lee, A. D., Mulroy, S. J., & Perry, J. Shoulder EMG during depression raise in men with spinal cord injury: The influence of lesion level. *The Journal of Spinal Cord Medicine*. 2003;26(1), 59–64.

Sharkey, N. A., & Marder, R. A. The rotator cuff opposes superior translation of the humeral head. *The American Journal of Sports Medicine*. 1995; 23(3), 270–275.

Shim, V., Boheme, J., Josten, C., Anderson, I. Use of Polyurethane Foam in Orthopaedic Biomechanical Experimentation and Simulation. *INTECH*. 2012

Slavens B. "Biomechanics," in *Handbook of Research on Biomedical Engineering Education and Advanced Bioengineering Learning: Interdisciplinary Concepts*. Eds. Ziad O. Abu-Faraj. Hershey, PA: Medical Information Science Reference, 2012, pp. 284-338.

Swieszkowski W , Bednarz P , Prendergast PJ . Contact stresses in the glenoid component in total shoulder arthroplasty . *Proc Inst Mech Eng*. 2003; 217 : 49 – 57 .

Terrier A., Merlini F., Pioletti D., Farron A. Total shoulder arthroplasty: downwards inclination of the glenoid component to balance supraspinatus deficiency. *Journal of Shoulder and Elbow Surgery*. 2009;18: 515–520.

Walch, G., Edwards, T.B., Boulahia, A., et al. The Infulence of glenohumeral prosthetic mismatch on glenoid radiolucent lines: results of a multicenter study. *Journal of Bone and Joint Surgery*. 2002 84A, 2186–2191.